

1 **Technical considerations in Hi-C scaffolding and evaluation of**
2 **chromosome-scale genome assemblies**

3

4 Kazuaki Yamaguchi^{1*}, Mitsutaka Kadota^{1*}, Osamu Nishimura^{1*}, Yuta Ohishi¹, Yuki

5 Naito², Shigehiro Kuraku^{1,3}

6

7 ¹Laboratory for Phyloinformatics, RIKEN Center for Biosystems Dynamics Research,

8 Kobe, Hyogo 650-0047, Japan, ²Database Center for Life Science (DBCLS), Mishima,

9 Shizuoka 411-8540, Japan, ³Molecular Life History Laboratory, National Institute of

10 Genetics, Mishima, Shizuoka 411-8540, Japan.

11

12 *These authors contributed equally to this study.

13 Correspondence address. Shigehiro Kuraku, Molecular Life History Laboratory,

14 National Institute of Genetics, Japan. Tel: +81 55 981 6801; Fax: +81 55 981 6801; E-

15 mail: skuraku@nig.ac.jp

16

17 Running title: On the chromosome-scale genome assembly

18

19 **Abstract**

20 The recent development of ecological studies has been fueled by the introduction of
21 massive information based on chromosome-scale genome sequences, even for
22 species for which genetic linkage is not accessible. This was enabled mainly by the
23 application of Hi-C, a method for genome-wide chromosome conformation capture that
24 was originally developed for investigating the long-range interaction of chromatins.
25 Performing genomic scaffolding using Hi-C data is highly resource-demanding and
26 employs elaborate laboratory steps for sample preparation. It starts with building a
27 primary genome sequence assembly as an input, which is followed by computation for
28 genome scaffolding using Hi-C data, requiring careful validation. This article presents
29 technical considerations for obtaining optimal Hi-C scaffolding results and provides a
30 test case of its application to a reptile species, the Madagascar ground gecko
31 (*Paroedura picta*). Among the metrics that are frequently used for evaluating
32 scaffolding results, we investigate the validity of the completeness assessment of
33 chromosome-scale genome assemblies using single-copy reference orthologs, and
34 report problems of the widely used program pipeline BUSCO.

35

36 **Keywords**

37 chromosome-scale genome assembly, Hi-C scaffolding, iconHi-C, gene space

38 completeness assessment, BUSCO

39

40 **Introduction**

41 Molecular ecology research often targets intra- or inter-specific variations of information
42 in DNA sequences. In eukaryotes, DNA molecules are found in cell nuclei as part of
43 “chromatin”, a complex of proteins that modulates the conformation of chromosomal
44 DNAs in the nuclear environment. Hi-C is a method for the genome-wide capture of
45 such chromosome conformations and was originally developed for detecting the long-
46 range interaction of chromatins (Lieberman-Aiden et al., 2009) (Figure 1). This method
47 has more recently been applied to the scaffolding of genome sequences from diverse
48 species (Burton et al., 2013; Kaplan & Dekker, 2013; Marie-Nelly et al., 2014). In
49 general, the more closely two genomic regions are located on DNA sequences, the
50 more frequently they contact in 3D genomes in chromatin. In genome scaffolding using
51 Hi-C data, fragmentary sequences of genomic DNA are grouped, ordered, and oriented
52 on the basis of chromatin contact frequency between different genomic regions.
53 Collectively, the genome scaffolding based on this type of chromatin contacts captured
54 *in situ* in nuclei by digestion-ligation (“proximity ligation”) is called proximity-guided
55 assembly (PGA).

56 Molecular ecology studies have been fueled by genome-wide approaches for
57 monitoring genetic diversity, which is most reliably achieved by the assembly of whole-

58 genome sequences using the output of modern DNA sequencers. Previously,
59 sequences resulting from whole-genome assembly were often flanked by long
60 interspersed repeats and remained unassembled with any other sequence (Peona,
61 Weissensteiner, & Suh, 2018). Under this circumstance, chromosome-scale sequences
62 were obtained only through genetic linkage mapping, which requires a cross of
63 identified mates and a sufficient number of offspring (Tang et al., 2015; Yoshitake et
64 al., 2018), or optical mapping, which requires a large quantity of high-molecular-weight
65 genomic DNA. After the introduction of PGA, Hi-C scaffolding has become a major
66 solution and has been adopted in mass genome sequencing projects to realize the
67 reconstruction of chromosome-scale sequences of genomic DNA (e.g., Rhie et al.,
68 2021).

69 The utility of Hi-C scaffolding is characterized by its handiness (compared with
70 the resource-demanding alternatives mentioned above), requiring only chromatin
71 preparation from a single individual and short-read sequencing on an ordinary
72 sequencing platform. Nonetheless, performing successful Hi-C scaffolding is not trivial.
73 Most frequently, researchers outsource the whole process to a commercial company or
74 an experienced collaborator, which may not allow them to optimize parameters
75 pertaining to sample preparation and computation with repeated attempts.

76 Alternatively, especially when cost-saving is desired, researchers may perform the
77 whole preparation by themselves; however, different parts of the process (tissue
78 sampling, library preparation, sequencing, scaffolding, and output validation) may be
79 performed by different individuals, rarely resulting in a self-contained experience. For
80 these reasons, technical tips regarding the whole process are not explicitly written or
81 shared with academic researcher communities, although they may accumulate at
82 facilities that take on mass genome sequencing projects. It should also be noted that
83 Hi-C requires the chromatin contained in cell nuclei, rather than extracted genomic
84 DNA. This is often misunderstood, even by those who have a long experience with
85 DNA sequencing, resulting in the unfavorable sampling and storage of materials.

86 In this review, we address the existing technical information about sample
87 preparation protocols/kits and computational programs, and present technical factors
88 for more successful Hi-C scaffolding (Figure 2) based on our experience with diverse
89 multicellular organisms (Kadota et al., 2020).

90

91 **What makes a difference in chromosome-scale genome scaffolding?**

92 The analysis of chromatin dynamics, for which Hi-C was originally developed, requires
93 appropriate tissues/cells as materials for addressing specific biological questions;

94 however, in Hi-C scaffolding, the choice of materials is less important because it
95 targets the reconstruction of the whole genome as the uniform goal, even when using
96 different cell populations in an organism. One may expect that the use of numerous
97 types of tissues will yield an optimal performance covering maximally diverse chromatin
98 contacts. However, our previous attempt with this intention did not lead to improvement
99 (Kadota et al., 2020). In general, the use of multiple tissues (in separate preparations)
100 should increase the chance of obtaining a more successful library, and it is preferable
101 to choose tissues with low endogenous nuclease activity and those from which single
102 cells can be prepared relatively easily for chromatin fixation. Table 1 summarizes the
103 key laboratory steps in the preparation of chromatin, Hi-C DNA, and libraries for
104 sequencing, in that order. As a non-commercial choice, this table includes the
105 traditional protocol by Rao et al. (2014), as well as a derivative of this protocol, iconHi-
106 C (Kadota et al., 2020), which resembles many others (e.g., Belagzhal et al., 2017). As
107 of April 2021, four biochemical companies (Arima Genomics, Dovetail Genomics,
108 Phase Genomics, and Qiagen) manufacture Hi-C kits, which are formulated with
109 different components and protocols. In general, conventional Hi-C kits employ a
110 restriction enzyme or a cocktail of multiple restriction enzymes, whereas Omni-C
111 employs a sequence-independent endonuclease (Table 1). In Omni-C, to capture more

112 proximal contacts, disuccinimidyl glutarate (DSG) and formaldehyde are used for
113 sample fixation (Nowak, Tian, & Brasier, 2005), which is now provided as a kit by
114 Dovetail Genomics. Restriction enzyme digestion and ligation are performed *in situ* or
115 on chromatin-binding beads. Library preparation is performed by sonication followed by
116 adapter ligation. The differences in specification between these kits/protocols include 1)
117 choice of the DNA digestion method, 2) method of biotin incorporation, 3) adaptability
118 of the sample quality control (QC) to the laboratory workflow, and 4) degree of
119 amplification in library preparation (Table 1). Sufficient attention to these factors will
120 issue an alert for unsuccessful sample preparation, such as insufficient chromatin
121 fixation and insufficient DNA digestion, and will allow the retrieval of chromatin contacts
122 with maximal diversity. Signs of unsuccessful samples will be alerted in QCs before
123 sequencing (Kadota et al., 2020). When a species of interest has unusual biochemical
124 properties in the selected tissues, genome size, and base composition, which affect the
125 efficiency and uniformity of DNA fragmentation, the choice of the kit/protocol may be
126 crucial (Figure 2).

127 Table 2 summarizes the specification of the existing computational programs for
128 Hi-C scaffolding. Most of these were developed and maintained by academic parties,
129 with the exception of HiRise, which is used exclusively in paid services by Dovetail

130 Genomics (Putnam et al., 2016), and LACHESIS, which is no longer maintained
131 (Burton et al., 2013). These programs implement different algorithms for using Hi-C
132 read alignment in scaffolding sequences (Ghurye et al., 2019). Apart from those core
133 algorithmic differences, more superficial parameters with default settings that vary
134 among programs can also largely affect the output, which includes a minimum input
135 sequence length (see Kadota et al., 2020 for an example of a remarkable improvement
136 using an altered length parameter setting) and the number of iterative cycles for misjoin
137 correction (Figure 2). Some of the programs listed in Table 2 are used with certain
138 specifications. FALCON-Phase (Kronenberg et al., 2018) requires the output of the
139 long read-based assembly by FALCON-Unzip (Chin et al., 2016), whereas ALLHiC,
140 which was developed to overcome the difficulty in resolving polyploidy, requires a
141 chromosome-scale genome assembly or an associated gene annotation for a closely
142 related species (Zhang, Zhang, Zhao, Ming, & Tang, 2019). More crucial key factors
143 that are independent of program choice include the quality and continuity of the input
144 genome assembly (reviewed in Whibley et al., 2020) and the amount of Hi-C reads
145 obtained after excluding improper fragments resulting from unintended ligation
146 products (self-ligation, re-ligation, and un-ligation (“dangling end”); see the details in
147 Kadota et al. (2020).

148 Overall, there is no single gold-standard method for library preparation and
149 post-sequencing scaffolding. When a need for troubleshooting is encountered, one can
150 consider the technical points included in Figure 2, which may provide alternatives for
151 possible improvement.

152

153 **Validation of chromosome-scale scaffolding output**

154 The goal of chromosome-scale genome assembly is the reconstruction of actual
155 nucleotide base lineups in DNA sequences. Assembly products can be rigidly
156 evaluated by referring to any independent information on genome size, chromosomal
157 organization, and location of individual genes, if available. It may not be widely known
158 that a Hi-C scaffolding output needs to be carefully evaluated and can often be
159 manually modified by referring to the matrix of chromatin contact frequencies (Howe et
160 al., 2020; also see below for an example of a reptile species), i.e., the process called
161 “review” in the manual of the program 3d-dna (<https://www.dnazoo.org/methods>). In Hi-
162 C scaffolding, inversions and misjoins occur more frequently than in other scaffolding
163 methods (Dudchenko et al., 2018; Ghurye et al., 2019). This is mainly because Hi-C
164 reads in pair do not instruct regarding the original fragment orientation in the genome,
165 and the orientation of the sequences that are to be joined is reliably determined only

166 when they are sufficiently long to harbor sufficient data points for chromatin contacts
167 among them and other sequences. Therefore, it is also important to choose a
168 scaffolding program that assumes and facilitates “review” in a dedicated editor, such as
169 JuiceBox (Dudchenko et al., 2018). The visualized chromatin contact map indicates the
170 parts to modify with outstanding signals distant from the diagonal line that do not fit in
171 the intensified signals (intra-chromosomal contacts) demarcated in squares (Figure
172 3a). Such outstanding signals caused by sequence misjoins or disjoins can be resolved
173 by relocating the relevant scaffolds in the contact map (e.g., Figure 3a and 3b). After
174 the “review”, HiC-Hiker can reduce the error rate further by considering not only the
175 junctions between two adjacent contigs, but also multiple neighboring contigs
176 (Nakabayashi & Morishita, 2020).

177 In reality, no comprehensive answer is available for checking the output of “*de*
178 *novo*” genome sequencing. However, karyotypes, namely the number and size of
179 chromosomes prepared from single cells, serve as valuable references for these
180 aspects, and should ideally be made available prior to the assessment of Hi-C
181 scaffolding results (see Uno et al., 2020 for an example of this sort for sharks with
182 scarce karyotyping reports). If chromosomal gene mapping records or optical mapping
183 results also exist, they can be used as a reference for validating the sequence

184 organization inside individual chromosomes. Several early studies employed an
185 existing genome assembly of a closely related species for validation (Dong et al., 2013;
186 Worley et al., 2014); however, this incurred uncontrollable risks because one cannot
187 discern the artifacts to be corrected from natural cross-species differences. It should be
188 noted that sex chromosome pairs (X/Y or Z/W) may not be assembled with high
189 precision, especially when they have regions that are similar to each other, which are
190 known as pseudoautosomal regions (PAR) (Liu et al., 2019). Another typical concern is
191 allelic redundancy. Unless one aims to separate different alleles (“haplotype phasing”),
192 it is advisable to discard highly similar sequences with allelic differences (“haplotigs”)
193 before performing Hi-C, because they can confuse Hi-C read mapping and result in
194 insufficient scaffolding in those regions.

195 Methods for evaluating large genome assemblies have been long debated, and
196 no single metric allows an overall assessment (Bradnam et al., 2013; Rhie et al., 2021;
197 Thrash, Hoffmann, & Perkins, 2020; Veeckman, Ruttink, & Vandepoele, 2016).

198 Scaffolding programs insert tracts of undetermined bases (“N”) between the sequences
199 joined by Hi-C data, and it should be noted that “N” is implicitly set to a uniform length
200 throughout a genome by individual programs (for example, inserting 500 Ns is the
201 default setting in 3d-dna and SALSA2).

202 In the evaluation of the output of *de novo* genome assembly, the metrics N50
203 length and NG50 length are frequently used (Bradnam et al., 2013). These metrics
204 apply to scaffold sequences and contig sequences, with the latter indicating sequences
205 without any intervening ambiguous bases (“N”). The N50 and NG50 length denotes the
206 length of the shortest sequence at 50% of the total sequence length in the genome
207 assembly and the genome size, respectively. Basically, a larger N50 or NG50 length
208 entails a more continuous genome assembly. However, the optimal N50 or NG50
209 length is inherently defined by the karyotype of the species of interest. For the human
210 genome, the N50 of the optimal genome assembly is approximately 154 Mbp, while it is
211 limited to approximately 15 Mbp for the sea lamprey, with more than 100 small, dot-like
212 chromosomes ($2n = 168$; Potter & Rothwell, 1970). For this unique karyotype, N50
213 length cannot be substantially larger than 15 Mbp. Even larger N50 lengths for this
214 species or its close relatives would indicate over-assembly, which can be the result of
215 the limited number of *in silico* chromosome fusions. Very importantly, the overall
216 sequence length statistics, such as N50 and NG50, do not reflect the sequence content
217 and its precision. To fulfill this task, one of the metrics proposed most recently was one
218 that quantifies the reconstruction of long terminal repeat (LTR) retrotransposons (LTR
219 Assembly Index, LAI) (Ou, Chen, & Jiang, 2018).

220 The demand for a more accurate assessment method is increasing as genome
221 sequences of unprecedented quality and continuity emerge. When evaluating genome
222 assemblies, one needs to perform a multi-faceted assessment using different metrics,
223 including the coverage of the protein-coding gene space, which is widely used as a
224 central metric (Figure 2). The following section will focus on how the use of the metric
225 for scoring the completeness of protein-coding genes should be adapted to the
226 prevailing chromosome-scale genome assembly production.

227

228 **Limitation of gene space completeness assessment—Who watches the**
229 **watchmen?**

230 The measurement of gene space completeness was used as a metric of genome
231 assembly quality even before 2010, when most of the available genome assemblies did
232 not reach a chromosomal scale. The only maintained program for this purpose in that
233 period, CEGMA (Parra, Bradnam, Ning, Keane, & Korf, 2009), was originally developed
234 for identifying a set of protein-coding genes in a given *de novo* genome assembly, to
235 be used as a gene set for training gene prediction programs (Parra, Bradnam, & Korf,
236 2007). Later, the support for CEGMA was discontinued, which was subsequently
237 almost completely replaced by BUSCO (Simão, Waterhouse, Ioannidis, Kriventseva, &

238 Zdobnov, 2015). Generally, when no other option is available as a benchmark solution,
239 users need to be warned about potential misleading reports from the single solution. As
240 previously reported for the benchmarking of multiple sequence alignments (Iantorno,
241 Gori, Goldman, Gil, & Dessimoz, 2014), developers and users of genome assembly
242 assessment tools should be fully informed about the perils of misleading assessments.

243 Since its first release in 2015, BUSCO has been rapidly upgraded to version 2
244 in 2016, version 3 in 2017, version 4 in 2019, and version 5 in January 2021. BUSCO
245 assumes the use of its accompanying gene set derived from OrthoDB (Kriventseva et
246 al., 2019), and both the gene set and the pipeline for searching reference genes have
247 been upgraded. This sort of benchmark program is expected to serve as a stable
248 standard on which the evaluation of genome assemblies is uniformly performed.
249 However, how can it provide a stable standard after such fast upgrading? Most
250 recently, the BUSCO pipeline was upgraded to version 5 and adopted a new
251 component program for gene search, MetaEuk (Levy Karin, Mirdita, & Söding, 2020),
252 which sometimes yields largely different values compared with the earlier versions 2
253 and 3 (these two versions superficially perform in the same way because version 3 was
254 a refactored version of version 2).

255 Another persistent concern with BUSCO is the criterion for choosing reference
256 single-copy genes (see Korlach et al., 2017)—genes that are absent from genome-
257 wide sequences of some species (no more than 10% of all of the species considered)
258 are included in the reference ortholog set. Some genes that were secondarily lost
259 during evolution can also be implicitly queried and judged as missing from the genome
260 assembly because of incomplete sequencing or assembly, which results in
261 underestimation of genome assembly completeness. Such an inaccurate assessment
262 of elaborately produced genome assemblies severely hampers the establishment of
263 reasonable decisions in research. To circumvent this systematic inaccuracy, we
264 previously developed a gene set (Core Vertebrate Genes, CVG) that contained only
265 the genes retained as single copies in all 29 rigorously selected vertebrate species
266 (Hara et al., 2015). This gene set is included as an option at our original web
267 application, gVolante (Nishimura, Hara, & Kuraku, 2017, 2019), in which different
268 BUSCO versions (including its latest version 5), as well as CEGMA, are available to
269 provide comparable metrics on a frozen standard.

270 Apart from the concerns mentioned above, scoring ortholog detection beyond
271 cross-species differences is not trivial. As a baseline that is independent of this factor,
272 we assessed the nearly complete human genome assembly CHM13 v1.0

273 (<https://github.com/nanopore-wgs-consortium/chm13>) released by the Telomere-to-
274 Telomere consortium (<https://sites.google.com/ucsc.edu/t2tworkinggroup/home>)—the
275 completeness assessment of this assembly is expected to be nearly 100% if no
276 technical limitations arise. This assessment of the human CHM13 v1.0 assembly
277 resulted in 79 genes judged as missing out of 5,310 BUSCO reference orthologs for
278 Tetrapoda (1.49%) by BUSCO version 5, and 1 out of 233 CVGs (0.43%) by CEGMA.
279 We tentatively analyzed the properties of these 79 reference genes that were judged
280 as missing in OrthoDB v9 and v10 and checked manually the nucleotide sequences of
281 the human CHM13 v1.0 genome assembly for the existence of their orthologs. Most
282 astonishingly, this search revealed that all 79 genes existed in the CHM13 v1.0
283 assembly (Table S1) and proved BUSCO's false-negative detections. This suggests a
284 systematic underestimation of completeness assessment scores by BUSCO, which
285 needs to be seriously considered, together with its continuous upgrading, which should
286 be explored further on a larger scale.

287 Importantly, in this human CHM13 genome assembly (version 1.0), the five
288 remaining gaps are known to be localized in non-protein-coding regions—more
289 precisely, ribosomal DNA arrays in the telomeric regions of five chromosomes. The
290 orthologs that were judged as missing in the assessment above are thought to have

291 escaped the gene detection process of the BUSCO pipeline. It is possible that such
292 false negatives occur when a queried ortholog is too divergent to fit within a range
293 recognized as an ortholog by BUSCO or has sequences that are too long or repetitive
294 (even in introns or flanking non-coding regions) to be scanned properly by the
295 programs implemented inside BUSCO, namely, TBLASTN and Augustus. This is a
296 remarkable example that shows the inaccuracy of completeness assessments using
297 reference orthologs. The inaccuracy is certainly mitigated by the use of thousands of
298 genes in an entire ortholog set; however, imprecise scores, especially those suggesting
299 a large missing portion, could be more seriously considered as we are obtaining
300 genome assemblies with maximal overall completeness.

301 Basically, genome assemblies with higher continuity are expected to yield
302 higher completeness scores (see Jauhal & Newcomb, 2020); however, the scores tend
303 to be rather saturated as long as the assessment targets the genomic space marked by
304 a limited number of protein-coding genes. Sometimes, the scores even decrease
305 slightly with increasing continuity when gene searches do not incorporate species-
306 specific features or are disturbed by insertion of the sequences (e.g., repetitive
307 elements) newly joined by Hi-C near exons. In resorting to protein-coding gene
308 completeness, one needs to pay closer attention to the mitigation of false negatives

309 and false positives, by choosing a more appropriate ortholog set and parameters for
310 ortholog search. It is also instrumental to perform an independent assessment of gene
311 coverage in genome assemblies by mapping raw RNA-seq reads or the transcript
312 contig sequences derived from them to the genome assembly sequences.

313

314 **Are they chromosomes?—Considerations in assembly finalization**

315 The typical practice of genome assembly finalization includes the process of removing
316 unnecessary sequences, such as unambiguous contaminants and organelle genomes.

317 Herein, a possible discrepancy between the number of resultant chromosome-scale
318 sequences and the haploid/diploid chromosome number needs to be addressed. This
319 should be followed by the renumbering of the sequences and other amendments
320 required at sequence submission to public databases

321 (<https://www.ncbi.nlm.nih.gov/genbank/genomesubmit/>). It remains controversial

322 whether the products of chromosome-scale genome assemblies can be called
323 “chromosomes”. A semantic criticism in this context is that chromosomes consist of not
324 only DNA, but also other components, mainly proteins. It should also be cautioned that
325 “chromosome-scale” sequences built by Hi-C scaffolding alone are prone to errors and
326 should be continuously improved by other approaches—it may be risky to regard “Hi-C

327 karyotyping” as replacing conventional cytogenetic analyses of karyotypes. To evoke a
328 careful distinction, a set of terms including “C-scaffold” (for chromosome-scale genome
329 scaffold, instead of “chromosome”) and “scaffotype” (a set of chromosome-scale
330 scaffolds, instead of “karyotype”) was introduced to avoid confusion (Lewin, Graves,
331 Ryder, Graphodatsky, & O'Brien, 2019). Apart from these concerns about semantics
332 and QC, the utility of chromosome-scale genome sequences opens up new frontiers of
333 molecular-level biology affecting a wide variety of fields involving diverse species
334 (reviewed in Deakin et al., 2019).

335

336 **Test case of the Madagascar ground gecko**

337 As a test case, we dissected the chromosome-scale genome assembly of the
338 Madagascar ground gecko (*Paroedura picta*) by referring to the technical consideration
339 factors raised above (Figure 2). The karyotype of this species is $2n = 36$ (Main,
340 Scantlebury, Zarkower, & Gamble, 2012), and the genome size based on the nuclear
341 DNA content is 1.80 Gbp (Hara et al., 2018). Molecular sequence data provision for
342 this animal was initiated with transcriptome analysis (Hara et al., 2015), which was
343 followed by short-read genome assembly (Hara et al., 2018). For loss-of-function
344 experiments, genome editing with CRISPR/Cas9 was recently demonstrated in a

345 reptilian species (Rasys et al., 2019). To promote the potential of this species in
346 question-driven biological studies, the genome assembly of this species has been
347 incorporated as one of the target species into the guide RNA designing tool
348 CRISPRdirect (<https://crispr.dbcls.jp/>) (Naito, Hino, Bono, & Ui-Tei, 2015). This
349 resource is expected to facilitate the use of this animal in diverse life science studies
350 that demand loss-of-function experiments.

351 The chromosome-scale genome scaffolding of the Madagascar ground gecko
352 benefited from the supply of embryos (see Supplemental Methods for the detailed
353 procedure). Chromatin preparation from the small embryonic sample allowed the
354 improvement of sequence continuity without sacrificing adult animals—the N50 scaffold
355 length increased from 4.1 to 109.0 Mbp (Table 3). This scaffolding performance was
356 achieved with only about 100 million read pairs, which is half of the data size usually
357 recommended in the specification of commercial kits (100 million read pairs per Gb of
358 genome). This could be because the diversity of the read obtained from our Hi-C library
359 was sufficiently high. Precise control of library quality before sequencing was a
360 prerequisite for this efficient data production (Figure S2).

361 As the input for this Hi-C scaffolding demonstration aimed at obtaining the first
362 chromosome-scale genome assembly for the taxon Gekkota, we employed three draft

363 genome assemblies: 1) the traditional short-read shotgun assembly; 2) the Chromium
364 supernova assembly using linked reads; and 3) the combination of the two former data
365 types, as well as scaffolding with paired-end RNA-seq reads (Figure S1). Each of these
366 three starting assemblies was scaffolded using Hi-C reads by varying the input
367 sequence length threshold, as included in Figure 2. We derived 15 chromosome-level
368 assemblies, and a total of 18 assemblies, including the three starting non-
369 chromosome-scale assemblies, were subjected to the comparison of sequence length
370 statistics and gene space completeness (Figure S3). Remarkably, varying input
371 sequence length thresholds largely affected the scaffolding output (Figure 3). From the
372 variable output, we identified an assembly with optimal or nearly optimal results
373 (Assembly 6 in Figures S2 and S3) regarding sequence length distribution (more
374 specifically, N50 scaffold length, largest scaffold length, and the proportion of the sum
375 scaffold length for the total assembly size). This assembly was subjected to manual
376 curation (“review”; see above), to derive a sequence assembly for a public release. The
377 manual interventions performed therein included a recovery of the linkage between two
378 small scaffolds, to form a putative single middle-sized chromosome sequence (Figure
379 3a,b). Importantly, in assessing the genome assembly of this species, a cross-species
380 comparison referring to a chromosome-scale genome assembly was not helpful,

381 because species outside the taxon Gekkota (e.g., anole lizard) diverged more than 150
382 million years ago (Hara et al., 2018). Conversely, our review was performed by
383 referring to the previously published records of gene mapping using fluorescence *in*
384 *situ* hybridization (FISH) on a different species of Gekkota (Supplemental Methods).

385 In the resulting assembly, the number of chromosome-scale scaffolds with a
386 length >1 Mbp was 18, which is almost the same as the haploid number of
387 chromosomes ($n = 18$ for XX/ZZ or 19 for XY/ZW; note that the sex chromosome
388 organization in this species is unknown) (Figure 3a). The percentage of sequences
389 longer than 1 Mbp in the entire assembly was 96.5%, indicating that most of the
390 sequence information is incorporated into the resulting chromosome-sized scaffolds
391 (Table 3). The resulting Madagascar ground gecko genome assembly was assessed to
392 cover 97.0% of the BUSCO's reference orthologs for the taxon Vertebrata (2,507 out of
393 2,586 genes) that were judged as being complete or fragmented by BUSCO version 5
394 (Table 3). The number of reference orthologs detected as complete increased by 2
395 genes after Hi-C scaffolding (Table 3).

396 The resulting chromosome-scale genome assembly of the Madagascar ground
397 gecko, which was introduced as an example of Hi-C scaffolding, will serve as a basis
398 for various studies focusing on the ecology and evolution of this species, as well as

399 other molecular-level biological studies performed in comparison with other amniote
400 species, including mammals and birds.

401

402 **Acknowledgments**

403 We thank the other members of the DNA Analysis Facility managed by the Laboratory
404 for Phyloinformatics, RIKEN BDR for daily collaboration, which provided the insights
405 outlined in this article, and Hiroshi Kiyonari for overall coordination of biological studies
406 on gecko. This work was supported by intramural grants from RIKEN, including the All-
407 RIKEN “Epigenome Manipulation Project”, and a Grant-in-Aid for Scientific Research
408 (B) from the Ministry of Education, Culture, Sports, Science and Technology (MEXT)
409 (20H03269) to SK.

410

411 **Author contributions**

412 SK conceived the study and drafted the manuscript. YO, SK, MK, ON, and KY
413 analyzed the data reviewed in this article. YN and KY set up public data use. All
414 authors contributed to the final writing of the manuscript.

415

416 **Data accessibility**

417 The Madagascar ground gecko genome assembly is available at Figshare
418 (<https://figshare.com/s/50a9a364c8dd45aa6af8>) and NCBI Genome under the
419 BioProject PRJDB5392.

420

421 **References**

422 Baudry, L., Guiguelmoni, N., Marie-Nelly, H., Cormier, A., Marbouty, M., Avia, K., . . .

423 Koszul, R. (2020). instaGRAAL: chromosome-level quality scaffolding of genomes

424 using a proximity ligation-based scaffold. *Genome Biol*, 21(1), 148.

425 doi:10.1186/s13059-020-02041-z

426 Belaghzal, H., Dekker, J., & Gibcus, J. H. (2017). Hi-C 2.0: An optimized Hi-C

427 procedure for high-resolution genome-wide mapping of chromosome conformation.

428 *Methods*, 123, 56-65. doi:10.1016/j.ymeth.2017.04.004

429 Bradnam, K. R., Fass, J. N., Alexandrov, A., Baranay, P., Bechner, M., Birol, I., . . .

430 Korf, I. F. (2013). Assemblathon 2: evaluating de novo methods of genome

431 assembly in three vertebrate species. *Gigascience*, 2(1), 10. doi:10.1186/2047-

432 217x-2-10

433 Burton, J. N., Adey, A., Patwardhan, R. P., Qiu, R., Kitzman, J. O., & Shendure, J.

434 (2013). Chromosome-scale scaffolding of de novo genome assemblies based on

435 chromatin interactions. *Nature Biotechnology*, 31(12), 1119-1125.
436 doi:10.1038/nbt.2727

437 Challis, R., Richards, E., Rajan, J., Cochrane, G., & Blaxter, M. (2020). BlobToolKit -
438 Interactive Quality Assessment of Genome Assemblies. *G3 (Bethesda)*, 10(4),
439 1361-1374. doi:10.1534/g3.119.400908

440 Chin, C. S., Peluso, P., Sedlazeck, F. J., Nattestad, M., Concepcion, G. T., Clum,
441 A., . . . Schatz, M. C. (2016). Phased diploid genome assembly with single-molecule
442 real-time sequencing. *Nature Methods*, 13(12), 1050-1054. doi:10.1038/nmeth.4035

443 Deakin, J. E., Potter, S., O'Neill, R., Ruiz-Herrera, A., Cioffi, M. B., Eldridge, M. D.
444 B., . . . Ezaz, T. (2019). Chromosomics: Bridging the Gap between Genomes and
445 Chromosomes. *Genes (Basel)*, 10(8). doi:10.3390/genes10080627

446 Dong, Y., Xie, M., Jiang, Y., Xiao, N., Du, X., Zhang, W., . . . Wang, W. (2013).
447 Sequencing and automated whole-genome optical mapping of the genome of a
448 domestic goat (*Capra hircus*). *Nature Biotechnology*, 31(2), 135-141.
449 doi:10.1038/nbt.2478

450 Dudchenko, O., Batra, S. S., Omer, A. D., Nyquist, S. K., Hoeger, M., Durand, N.
451 C., . . . Aiden, E. L. (2017). De novo assembly of the *Aedes aegypti* genome using

452 Hi-C yields chromosome-length scaffolds. *Science*, 356(6333), 92-95.
453 doi:10.1126/science.aal3327

454 Dudchenko, O., Shamim, M. S., Batra, S. S., Durand, N. C., Musial, N. T., Mostofa,
455 R., . . . Aiden, E. L. (2018). The Juicebox Assembly Tools module facilitates de novo
456 assembly of mammalian genomes with chromosome-length scaffolds for under
457 \$1000. *bioRxiv*, 254797. doi:10.1101/254797

458 Durand, N. C., Shamim, M. S., Machol, I., Rao, S. S., Huntley, M. H., Lander, E. S., &
459 Aiden, E. L. (2016). Juicer Provides a One-Click System for Analyzing Loop-
460 Resolution Hi-C Experiments. *Cell Syst*, 3(1), 95-98. doi:10.1016/j.cels.2016.07.002

461 Ghurye, J., Rhie, A., Walenz, B. P., Schmitt, A., Selvaraj, S., Pop, M., . . . Koren, S.
462 (2019). Integrating Hi-C links with assembly graphs for chromosome-scale
463 assembly. *PLoS Comput Biol*, 15(8), e1007273. doi:10.1371/journal.pcbi.1007273

464 Hara, Y., Takeuchi, M., Kageyama, Y., Tatsumi, K., Hibi, M., Kiyonari, H., & Kuraku, S.
465 (2018). Madagascar ground gecko genome analysis characterizes asymmetric fates
466 of duplicated genes. *BMC Biology*, 16(1), 40. doi:10.1186/s12915-018-0509-4

467 Hara, Y., Tatsumi, K., Yoshida, M., Kajikawa, E., Kiyonari, H., & Kuraku, S. (2015).
468 Optimizing and benchmarking de novo transcriptome sequencing: from library

469 preparation to assembly evaluation. *BMC Genomics*, 16, 977. doi:10.1186/s12864-
470 015-2007-1

471 Howe, K., Chow, W., Collins, J., Pelan, S., Pointon, D.-L., Sims, Y., . . . Wood, J.
472 (2020). Significantly improving the quality of genome assemblies through curation.
473 *bioRxiv*, 2020.2008.2012.247734. doi:10.1101/2020.08.12.247734

474 Iantorno, S., Gori, K., Goldman, N., Gil, M., & Dessimoz, C. (2014). Who watches the
475 watchmen? An appraisal of benchmarks for multiple sequence alignment. *Methods*
476 *Mol Biol*, 1079, 59-73. doi:10.1007/978-1-62703-646-7_4

477 Jauhal, A. A., & Newcomb, R. D. (2021). Assessing genome assembly quality prior to
478 downstream analysis: N50 versus BUSCO. *Mol Ecol Resour*. doi:10.1111/1755-
479 0998.13364

480 Kadota, M., Nishimura, O., Miura, H., Tanaka, K., Hiratani, I., & Kuraku, S. (2020).
481 Multifaceted Hi-C benchmarking: what makes a difference in chromosome-scale
482 genome scaffolding? *Gigascience*, 9(1). doi:10.1093/gigascience/giz158

483 Kaplan, N., & Dekker, J. (2013). High-throughput genome scaffolding from in vivo DNA
484 interaction frequency. *Nature Biotechnology*, 31(12), 1143-1147.
485 doi:10.1038/nbt.2768

486 Korlach, J., Gedman, G., Kingan, S. B., Chin, C. S., Howard, J. T., Audet, J. N., . . .
487 Jarvis, E. D. (2017). De novo PacBio long-read and phased avian genome
488 assemblies correct and add to reference genes generated with intermediate and
489 short reads. *Gigascience*, 6(10), 1-16. doi:10.1093/gigascience/gix085

490 Kriventseva, E. V., Kuznetsov, D., Tegenfeldt, F., Manni, M., Dias, R., Simão, F. A., &
491 Zdobnov, E. M. (2019). OrthoDB v10: sampling the diversity of animal, plant, fungal,
492 protist, bacterial and viral genomes for evolutionary and functional annotations of
493 orthologs. *Nucleic Acids Research*, 47(D1), D807-d811. doi:10.1093/nar/gky1053

494 Kronenberg, Z. N., Hall, R. J., Hiendleder, S., Smith, T. P. L., Sullivan, S. T., Williams,
495 J. L., & Kingan, S. B. (2018). FALCON-Phase: Integrating PacBio and Hi-C data for
496 phased diploid genomes. *bioRxiv*, 327064. doi:10.1101/327064

497 Levy Karin, E., Mirdita, M., & Söding, J. (2020). MetaEuk-sensitive, high-throughput
498 gene discovery, and annotation for large-scale eukaryotic metagenomics.
499 *Microbiome*, 8(1), 48. doi:10.1186/s40168-020-00808-x

500 Lewin, H. A., Graves, J. A. M., Ryder, O. A., Graphodatsky, A. S., & O'Brien, S. J.
501 (2019). Precision nomenclature for the new genomics. *Gigascience*, 8(8).
502 doi:10.1093/gigascience/giz086

503 Lieberman-Aiden, E., van Berkum, N. L., Williams, L., Imakaev, M., Ragoczy, T.,
504 Telling, A., . . . Dekker, J. (2009). Comprehensive mapping of long-range
505 interactions reveals folding principles of the human genome. *Science*, *326*(5950),
506 289-293. doi:10.1126/science.1181369

507 Liu, R., Low, W. Y., Tearle, R., Koren, S., Ghurye, J., Rhie, A., . . . Williams, J. L.
508 (2019). New insights into mammalian sex chromosome structure and evolution
509 using high-quality sequences from bovine X and Y chromosomes. *BMC Genomics*,
510 *20*(1), 1000. doi:10.1186/s12864-019-6364-z

511 Main, H., Scantlebury, D. P., Zarkower, D., & Gamble, T. (2012). Karyotypes of two
512 species of Malagasy ground gecko (Paroedura: Gekkonidae). *African Journal of*
513 *Herpetology*, *61*(1), 81-90. doi:10.1080/21564574.2012.667837

514 Marie-Nelly, H., Marbouty, M., Cournac, A., Flot, J. F., Liti, G., Parodi, D. P., . . .
515 Koszul, R. (2014). High-quality genome (re)assembly using chromosomal contact
516 data. *Nat Commun*, *5*, 5695. doi:10.1038/ncomms6695

517 Naito, Y., Hino, K., Bono, H., & Ui-Tei, K. (2015). CRISPRdirect: software for designing
518 CRISPR/Cas guide RNA with reduced off-target sites. *Bioinformatics*, *31*(7), 1120-
519 1123. doi:10.1093/bioinformatics/btu743

520 Nakabayashi, R., & Morishita, S. (2020). HiC-Hiker: a probabilistic model to determine
521 contig orientation in chromosome-length scaffolds with Hi-C. *Bioinformatics*, 36(13),
522 3966-3974. doi:10.1093/bioinformatics/btaa288

523 Nishimura, O., Hara, Y., & Kuraku, S. (2017). gVolante for standardizing completeness
524 assessment of genome and transcriptome assemblies. *Bioinformatics*, 33(22), 3635-
525 3637. doi:10.1093/bioinformatics/btx445

526 Nishimura, O., Hara, Y., & Kuraku, S. (2019). Evaluating Genome Assemblies and
527 Gene Models Using gVolante. *Methods Mol Biol*, 1962, 247-256. doi:10.1007/978-1-
528 4939-9173-0_15

529 Nowak, D. E., Tian, B., & Brasier, A. R. (2005). Two-step cross-linking method for
530 identification of NF-kappaB gene network by chromatin immunoprecipitation.
531 *BioTechniques*, 39(5), 715-725. doi:10.2144/000112014

532 Ou, S., Chen, J., & Jiang, N. (2018). Assessing genome assembly quality using the
533 LTR Assembly Index (LAI). *Nucleic Acids Research*, 46(21), e126.
534 doi:10.1093/nar/gky730

535 Parra, G., Bradnam, K., & Korf, I. (2007). CEGMA: a pipeline to accurately annotate
536 core genes in eukaryotic genomes. *Bioinformatics*, 23(9), 1061-1067.
537 doi:10.1093/bioinformatics/btm071

538 Parra, G., Bradnam, K., Ning, Z., Keane, T., & Korf, I. (2009). Assessing the gene
539 space in draft genomes. *Nucleic Acids Research*, 37(1), 289-297.
540 doi:10.1093/nar/gkn916

541 Peona, V., Weissensteiner, M. H., & Suh, A. (2018). How complete are "complete"
542 genome assemblies?-An avian perspective. *Mol Ecol Resour*, 18(6), 1188-1195.
543 doi:10.1111/1755-0998.12933

544 Potter, I. C., & Rothwell, B. (1970). The mitotic chromosomes of the lamprey,
545 *Petromyzon marinus* L. *Experientia*, 26(4), 429-430. doi:10.1007/bf01896930

546 Putnam, N. H., O'Connell, B. L., Stites, J. C., Rice, B. J., Blanchette, M., Calef, R., . . .
547 Green, R. E. (2016). Chromosome-scale shotgun assembly using an in vitro method
548 for long-range linkage. *Genome Research*, 26(3), 342-350.
549 doi:10.1101/gr.193474.115

550 Rao, S. S., Huntley, M. H., Durand, N. C., Stamenova, E. K., Bochkov, I. D., Robinson,
551 J. T., . . . Aiden, E. L. (2014). A 3D map of the human genome at kilobase resolution
552 reveals principles of chromatin looping. *Cell*, 159(7), 1665-1680.
553 doi:10.1016/j.cell.2014.11.021

554 Rasys, A. M., Park, S., Ball, R. E., Alcalá, A. J., Lauderdale, J. D., & Menke, D. B.
555 (2019). CRISPR-Cas9 Gene Editing in Lizards through Microinjection of Unfertilized
556 Oocytes. *Cell Rep*, 28(9), 2288-2292 e2283. doi:10.1016/j.celrep.2019.07.089

557 Renschler, G., Richard, G., Valsecchi, C. I. K., Toscano, S., Arrigoni, L., Ramírez, F., &
558 Akhtar, A. (2019). Hi-C guided assemblies reveal conserved regulatory topologies
559 on X and autosomes despite extensive genome shuffling. *Genes & Development*,
560 33(21-22), 1591-1612. doi:10.1101/gad.328971.119

561 Rhie, A., McCarthy, S. A., Fedrigo, O., Damas, J., Formenti, G., Koren, S., . . . Jarvis,
562 E. D. (2021). Towards complete and error-free genome assemblies of all vertebrate
563 species. *Nature*, 592(7856), 737-746. doi:10.1038/s41586-021-03451-0

564 Simão, F. A., Waterhouse, R. M., Ioannidis, P., Kriventseva, E. V., & Zdobnov, E. M.
565 (2015). BUSCO: assessing genome assembly and annotation completeness with
566 single-copy orthologs. *Bioinformatics*, 31(19), 3210-3212.
567 doi:10.1093/bioinformatics/btv351

568 Tang, H., Zhang, X., Miao, C., Zhang, J., Ming, R., Schnable, J. C., . . . Lu, J. (2015).
569 ALLMAPS: robust scaffold ordering based on multiple maps. *Genome Biol*, 16(1), 3.
570 doi:10.1186/s13059-014-0573-1

571 Thrash, A., Hoffmann, F., & Perkins, A. (2020). Toward a more holistic method of
572 genome assembly assessment. *BMC Bioinformatics*, 21(Suppl 4), 249.
573 doi:10.1186/s12859-020-3382-4

574 Uno, Y., Nozu, R., Kiyatake, I., Higashiguchi, N., Sodeyama, S., Murakumo, K., . . .
575 Kuraku, S. (2020). Cell culture-based karyotyping of orectolobiform sharks for
576 chromosome-scale genome analysis. *Commun Biol*, 3(1), 652. doi:10.1038/s42003-
577 020-01373-7

578 Veeckman, E., Ruttink, T., & Vandepoele, K. (2016). Are We There Yet? Reliably
579 Estimating the Completeness of Plant Genome Sequences. *Plant Cell*, 28(8), 1759-
580 1768. doi:10.1105/tpc.16.00349

581 Whibley, A., Kelley, J. L., & Narum, S. R. (2021). The changing face of genome
582 assemblies: Guidance on achieving high-quality reference genomes. *Mol Ecol*
583 *Resour*, 21(3), 641-652. doi:10.1111/1755-0998.13312

584 Worley, K. C., Warren, W. C., Rogers, J., Locke, D., Muzny, D. M., Mardis, E. R., . . .
585 Analysis, C. (2014). The common marmoset genome provides insight into primate
586 biology and evolution. *Nature Genetics*, 46(8), 850-857. doi:10.1038/ng.3042

587 Yoshitake, K., Igarashi, Y., Mizukoshi, M., Kinoshita, S., Mitsuyama, S., Suzuki, Y., . . .
588 Asakawa, S. (2018). Artificially designed hybrids facilitate efficient generation of

589 high-resolution linkage maps. *Sci Rep*, 8(1), 16104. doi:10.1038/s41598-018-34431-

590 6

591 Zhang, X., Zhang, S., Zhao, Q., Ming, R., & Tang, H. (2019). Assembly of allele-aware,

592 chromosomal-scale autopolyploid genomes based on Hi-C data. *Nat Plants*, 5(8),

593 833-845. doi:10.1038/s41477-019-0487-8

594

TABLE 1 Comparison of sample preparation for proximity-based genome scaffolding.

Different specifications	<i>In situ</i> Hi-C by Rao et al. ^a	iconHi-C (ver. 1.0) ^b	Arima-HiC Kit (Arima Genomics; ver. A160134 v01)	Proximo Hi-C (Animal) Prep Kit (Phase Genomics; ver. 4.0)	Dovetail Hi-C Kit (Dovetail Genomics; ver. 1.4)	Omni-C Proximity Ligation Assay Kit (Dovetail Genomics; ver. 1.3)	EpiTect Hi-C Kit (Qiagen; ver. 04/2019)
Crosslinking agent	Formaldehyde (final 1%)	Formaldehyde (final 1%)	Formaldehyde (final 2%)	Crosslinking solution (included in the kit)	Formaldehyde (final 1.5%)	DSG (final 30 mM) ^c and formaldehyde (final 1%)	Formaldehyde (final 1%)
Enzyme for chromatin DNA digestion	Mbol (cuts at "GATC")	HindIII (cuts at "AAGCTT") or DpnII (cuts at "GATC")	Cocktail of A1 and A2 enzymes (cut at "GATC" and "GANTC") ^c	Sau3AI (cuts at "GATC")	DpnII (cuts at "GATC")	Nuclease enzyme mix ^c	Hi-C digestion enzyme (cuts at "GATC")
Duration of restriction enzyme digestion	2 h to overnight at 37°C	Overnight at 37°C	30–60 min at 37°C	1 h at 37°C	1 h at 37°C	30 min at 30°C	2 h at 37°C
Biotin-labeling method	Incorporation of biotinylated nucleotide	Incorporation of biotinylated nucleotide	Incorporation of biotinylated nucleotide	Incorporation of biotinylated nucleotide	Incorporation of biotinylated nucleotide	Ligation of biotin-containing bridge adapter ^c	Incorporation of biotinylated nucleotide
Chromatin capture	N/A	N/A	N/A	By Recovery Beads (included in the kit) ^c	By Chromatin Capture Beads (included in the kit) ^c	By Chromatin Capture Beads (included in the kit) ^c	N/A
Ligation condition	4 h at room temperature	4–6 h at 16°C	15 min at room temperature	4 h at 25°C	1–16 h at 16°C	30 min at 22°C and 1 h at 22°C ^c	2 h at 16°C
Reverse crosslinking	Overnight or at least 1.5 h at 68°C	Overnight at 65°C	1.5–16 h at 68°C	1–18 h at 65°C	45 min at 68°C	45 min at 68°C	90 min at 80°C ^c
Quality control (QC) of ligated DNA	No	Yes (by size distribution analysis)	Yes (yield of biotin incorporated DNA)	Yes (yield of biotin incorporated DNA)	Yes (yield of ligated DNA)	Yes (yield of ligated DNA)	No

Removal of biotin from unligated ends	No	Yes	No	No	No	N/A	No
PCR cycles for sequencing library preparation	4–12 cycles	Optimized for each library ^c	Optimized for each library ^c	12 cycles	11 cycles	12 cycles	7 cycles
Library QC target	Not specified	Yield and size distribution; digestion with NheI or ClaI ^c	Yield and size distribution	Yield and size distribution	Yield and size distribution	Yield and size distribution	Yield and size distribution

^aRao et al. 2014; ^bKadota et al., 2020; ^cSpecification applied to a subset of the kits/protocols.

597 **TABLE 2** Comparison of computational programs for proximity-based genome scaffolding. The programs are sorted in the descending order of
 598 the number of citations in the literature introducing the individual programs, with the exception of the programs that are not openly maintained
 599 (LACHESIS and HiRise at the bottom).

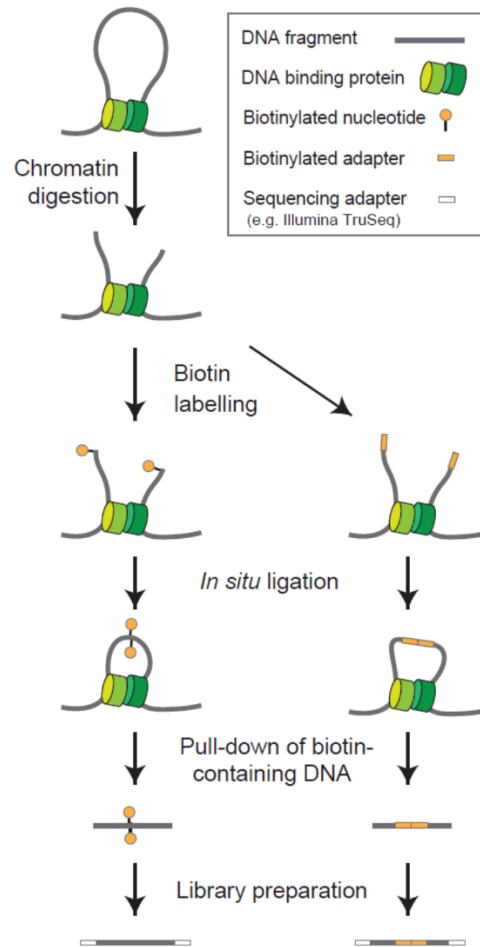
Program	Description	Input data requirement	Other information
3d-dna ^{a,b}	Misjoin correction algorithm is applied to detect errors in the input assembly; compatible with multiple enzymes	Accepts only Juicer mapper format	The results can be reviewed and modified directly by JuiceBox
SALSA2 ^c	Uses the physical coverage of Hi-C pairs to identify misassembled regions of the input assembly; compatible with multiple enzymes	Generic bam (bed) file, assembly graph, unitig, 10x link files	The results can be reviewed and modified by JuiceBox via the included script
ALLHiC ^d	Scaffolding and phasing of a polyploid genome	Hi-C read pairs; (option) associated gene annotation or chromosome-scale genome assembly for a closely related species	Generate the chromatin contact matrix to evaluate genome scaffolding
FALCON-Phase ^e	Scaffolding and phasing of a diploid genome	Hi-C read pairs; FALCON-Unzip assembly	Output two phased full-length pseudo-haplotypes
HiCAssembler ^f	Misassemblies are corrected by iterative joining of high-confidence scaffold paths	Hi-C matrix of h5 format created by HiCExplorer	Misassembled regions in the input assembly can be corrected by specifying the location in the program
instaGRAAL ^g	Overhauling the GRAAL program to allow efficient assembly of large genomes	Hi-C matrix of instaGRAAL format created by hicstuff or HiC-Box	Requires NVIDIA CUDA and can be executed in a limited environment
LACHESIS ^h	No function to correct scaffold misjoins	Generic bam format	Developer's support discontinued; intricate installation
HiRise ⁱ	Employed in Dovetail Chicago/Hi-C service	Generic bam format	Open-source version at GitHub not updated since 2015

600 ^aDudchenko et al., 2017; ^bDurand et al., 2016; ^cGhurye et al., 2019; ^dZhang et al., 2019; ^eKronenberg et al., 2018; ^fRenschler et al., 2019; ^gBaudry et al.,
 601 2020; ^hBurton et al., 2013; ⁱPutnam et al., 2016.

602 **TABLE 3** Improvement of the Madagascar ground gecko genome assembly. BUSCO's
 603 Tetrapoda gene set consisting of 5310 orthologs was used to assess gene space
 604 completeness with BUSCO v5.
 605

Metric	Draft v1.0 (Hara et al., 2018)	Hi-C scaffolds v2.0 (This study)
Total length (Mbp)	1,694	1,562
N50 scaffold length (Mbp)	4.1	109.0
Largest scaffold length (Mbp)	33.7	184.3
# of scaffolds >1 Mbp	297	18
% of sum length of sequences >10 Mbp	26.6	96.5
% of sum length of sequences >1 Mbp	73.3	96.5
# (%) of reference orthologs detected as "complete"	4,575 (86.16%)	4,577 (86.20%)
# (%) of reference orthologs detected as 'fragmented' or "complete"	4,960 (93.41%)	4,969 (93.58%)
# (%) of reference orthologs detected as "duplicated"	45 (0.8%)	38 (0.7%)
# (%) of reference orthologs recognized as "missing"	350 (6.59%)	341 (6.42%)

606
 607
 608



609

610 **FIGURE 1** Overview of the workflow used for Hi-C library preparation. Digestion of chromatin DNA is
 611 performed with restriction enzymes or DNA nuclease. DNA ends are labeled by a biotinylated
 612 nucleotide (left) or a biotinylated bridge adapter (right). Ligation is performed *in situ* in the nucleus,
 613 and biotin-containing DNA is captured and used for the generation of sequencing libraries.

614

615

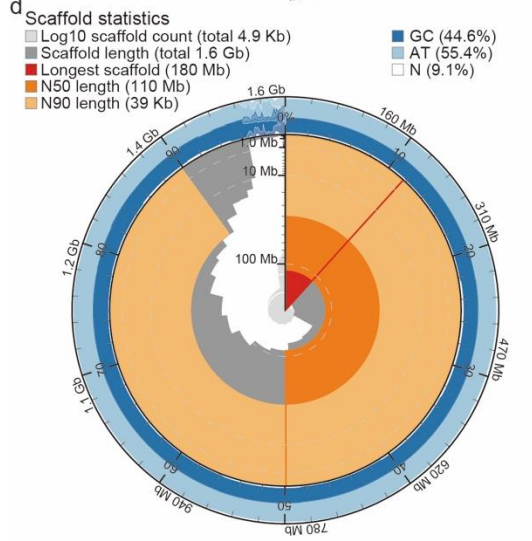
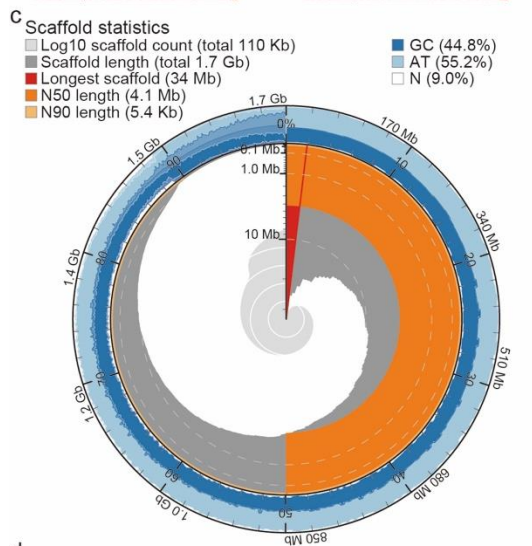
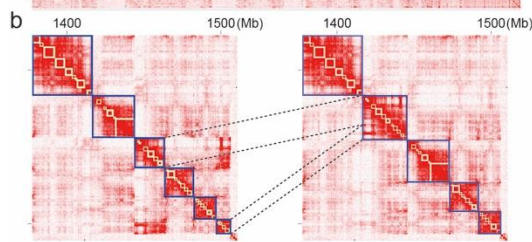
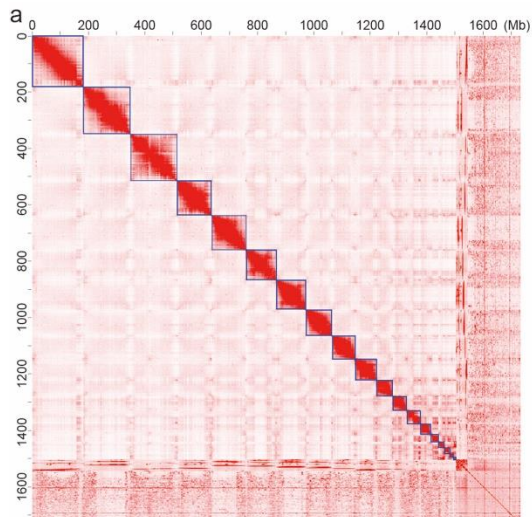
	Consideration factor	Possible solution	Test case with gecko
Sampling	Avoid cell population with high nuclease activity Cell cycle status may affect contact profiles	Process multiple tissues	Whole embryo at stage 28
Hi-C DNA preparation	DNA digestion may result in regional bias Stay alarmed with unsuccessful preparation	Use a different enzyme or a Hi-C protocol/kit Perform QC suitable for DNA digestion method	HindIII employed in the iconHi-C protocol QC for DNA length distribution performed
Library preparation	Avoid overamplification to increase read diversity Stay alarmed with unsuccessful preparation	Perform PCR after optimizing the cycle number Perform QC suitable for DNA digestion method	Five PCR cycles after a preliminary PCR QC with RE digestion performed
Sequencing	Low read diversity incurs a large cost	Preliminary small-scale sequencing in advance	Approx. 100 million paired-end reads sequenced
Hi-C data processing	Achieve unique read mapping	Rigidly select authentic Hi-C read pairs	HiC-Pro and Juicer
Scaffolding	Which computational program to choose? Length threshold setting for input sequences Iteration for misjoin correction	Promising choices in Table 2 Test multiple parameters Test multiple parameters	3d-dna Variable parameters (1, 3, 5, 10, and 15 kb) Two rounds of misjoin correction
Evaluation	How many scaffolds are chromosome-scale? Is the protein-coding landscape widely covered? Are the non-coding regions widely covered? Is any sex chromosome included in the assembly?	Length distribution analysis in light of karyotype Gene space completeness assessment Other metrics (e.g. synteny, LTR Assembly Index) Quantify male/female coverage ratio	Assessment on the gVolante webserver Assessment on the gVolante webserver Confirmed high cross-species linkage similarity Unresolved because of insufficient information
Curation	Resembles the karyotype? Are haplotypes phased?	'Review' the chromatin contact map Purge or resolve duplicated scaffolds	Manual curation on Juicebox Confirmed minimal duplication with BUSCO

616

617 **FIGURE 2** Technical considerations in Hi-C scaffolding. The major points regarding technical considerations (left) are shown as hands-on

618 steps. Individual rows show possible solutions (middle) and our demonstration using the Madagascar ground gecko (right).

619



621

622

623 **FIGURE 3** Genome assembly of the Madagascar ground gecko. (a) Hi-C contact map. The
624 intensities of chromatin contacts quantified in Hi-C data (red) are indicated in the matrix of
625 different genomic regions. The blue frames indicate the putative chromosomal units. (b) An
626 example of manual curation. The white frames indicate the scaffold units before Hi-C
627 scaffolding. In a part of the magnified view of the contact map shown in (a), the two input
628 scaffolds indicated by the dashed lines on the left were judged to be derived from a single
629 scaffold on the right. (c, d) Snail plots of the genome assembly before (c) and after (d) Hi-C
630 scaffolding. These plots were produced using BlobTools2 (Challis, Richards, Rajan,
631 Cochrane, & Blaxter, 2020). The light-gray spiral at the center shows the cumulative record
632 count on a log scale, with the white lines indicating successive orders of digits. The
633 distribution of scaffold lengths is shown in dark gray with the plot radius scaled to the longest
634 scaffold of the assembly, and the ranges in orange and light orange indicate the N50 and
635 N90 lengths, respectively. The blue area in the outer layer shows the distribution of GC, AT,
636 and N percentages in the base composition of each scaffold unit.